CAUSAL GRAPH NEURAL NETWORKS FOR WILDFIRE DANGER PREDICTION

Shan Zhao[1], **Ioannis Prapas**[2,3], **Ilektra Karasante**[2], **Zhitong Xiong**[1], **Ioannis Papoutsis**[2], **Gustau Camps-Valls**[3], **Xiao Xiang Zhu**[1]
[1] Technical University of Munich, Ottobrunn, 85521, Germany
[2] National Observatory of Athens, Athens, 11810, Greece
[3] University of València, Valencia, 46980, Spain

ABSTRACT

Wildfire forecasting is notoriously hard due to the complex interplay of different factors such as weather conditions, vegetation types and human activities. Deep learning models show promise in dealing with this complexity by learning directly from data. However, to inform critical decision making, we argue that we need models that are right for the right reasons; that is, the implicit rules learned should be grounded by the underlying processes driving wildfires. In that direction, we propose integrating causality with Graph Neural Networks (GNNs) that explicitly model the causal mechanism among complex variables via graph learning. The causal adjacency matrix considers the synergistic effect among variables and removes the spurious links from highly correlated impacts. Our methodology's effectiveness is demonstrated through superior performance forecasting wildfire patterns in the European boreal and mediterranean biome. The gain is especially prominent in a highly imbalanced dataset, showcasing an enhanced robustness of the model to adapt to regime shifts in functional relationships. Furthermore, SHAP values from our trained model further enhance our understanding of the model's inner workings.

1 INTRODUCTION

Wildfires present considerable risks to human safety and economic stability in affected regions and wildlife habitats. The risk is inflated by climate change, which aggravates wildfires, particularly in the vulnerable european ecosystems that this study targets (Batllori et al., 2013). Accurately predicting the highly favorable conditions for a wildfire is vital for effective disaster prevention and preparedness. Earth observation data is pivotal in fire danger assessment and forecasting, offering extensive meteorological and vegetation condition information closely related to wildfire occurrences (Pettinari & Chuvieco, 2020). The copious amount of data available lends itself well to sophisticated deep learning (DL) approaches (Camps-Valls et al., 2021; Reichstein et al., 2019) for predicting wildfire danger (Prapas et al., 2021). Recent advancements have been made by taking multiple factors as model inputs. Li et al. (2023) underscore the importance of delayed interactions between wildfires and climate patterns in the forecasting scenarios. Kondylatos et al. (2022) identified the most critical predictors of the next day's wildfire danger using explainable AI (xAI) methods. TeleVit (Prapas et al., 2023) incorporates different local, global variables with teleconnection indices within a transformer-based architecture. However, these approaches do not explicitly model the information flow within the model. Consequently, the mechanism of how the variables interact and assist the final prediction is not considered during the model design and training procedure.

The application of causal inference in Remote Sensing enhances our understanding of processes in the Earth system and facilitates effective interventions (Runge et al., 2023; Camps-Valls et al., 2023). Pérez-Suay & Camps-Valls (2018) propose an asymmetry-based approach that uses sensitivity criterion to address the causal direction between geoscientific variables. State-space method CCM (Tsonis et al., 2018) finds its applications in Ecosystem (Sugihara et al., 2012), land-atmosphere interactions (Wang et al., 2018; Díaz et al., 2022), and identifying influencing factors in urban soil pollutants (Gao et al., 2023). Integrating causal inference with DL architectures remains challenging

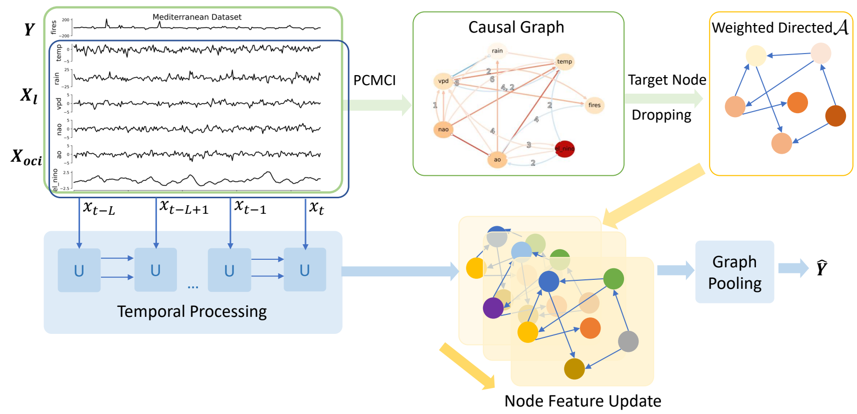

Figure 1: Workflow of our proposed Causal-GNN. The inputs contain local and OCI variables with various temporal and spatial scales. The adjacency matrix captures the causal relationship among variables. The node feature is extracted by the temporal module and updated via GNNs for the final prediction. The cross-entropy between the prediction and ground truth is minimized.

due to the gap between the low-level inputs (e.g. images or earth observation data) and high-level definitions of graphic nodes. ANM (Zhang & Hyvarinen, 2012) uses Multi-layer Perceptions to estimate the nonlinear causal effects between variables. Iglesias-Suarez et al. (2023) propose a Causal Neural Network (NN) to improve climate projection. However, most efforts are limited to feature selection and observational data regression.

Intricate causal relationship modeling among variables can support robust and reliable DL (Schölkopf et al., 2021; Varando et al., 2021). In this work, we incorporate a causality graph into the GNN architecture, thereby capturing the information flow through graph learning techniques. Our experimental results reveal that the causality-infused graph is a robust indicator of pertinent information, enhancing prediction quality. The SHapley Additive exPlanations (SHAP) (Lundberg & Lee, 2017) values derived from our model reveal the memory effect of teleconnections in driving the wildfire danger.

2 Methods

In the Earth system, *Synergistic Effects* (Runge et al., 2019a) are the combined effects of drivers making an impact that is greater than the simple sum of its parts. For instance, devastating wildfires are often related to dryness conditions, combustible materials, and an ignition source, but their impacts are subjected to threshold behavior (Reichstein et al., 2013). Causal methods allow us to identify regime shifts in functional relationships triggered by extreme conditions (Runge et al., 2019a). We consider leveraging the causal graph and the message passing of a temporal GNN to capture the wildfire dynamics.

Given an input of local scale variables $X_l \in \mathbb{R}^{B \times C_l \times L_l}$ and Oceanic and Climatic Indices (OCIs) variables $X_{oci} \in \mathbb{R}^{B \times C_{oci} \times L_{oci}}$, where B is the batch size, C is the number of variables, and L is the time lag to the current time step t, our task is to predict the wildfire danger $Y \subset \{0, 1\} \in \mathbb{R}^B$ in the future time step $t + h$, where h is the forecasting horizon.

GNNs extend DL to data with a graph structure. The two key components of GNNs are the adjacency matrix and node features. Given that causality is usually represented with graphs (Runge et al., 2019b), we create this adjacency matrix $\mathcal{A} \in \mathcal{R}^{(C_l+C_{oci})\times(C_l+C_{oci})}$ from a causal graph. The strength of the causal link quantifies weights of $\mathcal{A}$. The causal graph is the graphic representation of the causal relationship among the variables. Our selection algorithm to compute the causal graph is the PCMCI method (Runge et al., 2019b). The nodes in the time series causal graph represent the variables X_t^j at different lag times, and $\mathcal{P}a(X_t^j) \in \mathbf{X}_t^- = \mathbf{X}_{t-1}, \mathbf{X}_{t-2}, ...$ denotes the causal parents of variable X_t^j. A causal link $X_{t-\tau}^i \rightarrow X_t^j$ exits if $X_{t-\tau}^i \in \mathcal{P}a(X_t^j)$. Multiple factors, such as a temporal trend, geographical shifts, and vegetation type, can introduce non-stationary dependencies that act as confounders. Thus, the data is preprocessed to ensure the causal stationarity.

The preprocessing is detailed in Appendix B.1. However, due to finite sample length and partially unfulfilled standard assumptions of causal discovery (Pearl, 2009; Spirtes et al., 2001), spurious links can still exist (Krich et al., 2020). To validate the findings with domain knowledge, we employ link assumptions (Appendix B.2) to orient parts of the edges.

Regarding the vertices in GNN, each node represents the temporal feature of the given variable, which is extracted by a single layer LSTM (Hochreiter & Schmidhuber, 1997). The node feature is updated by message transmission among neighboring nodes whose connectivity is defined within the adjacency matrix. The node feature is refined via multiple convolution layers with layer norm and activation. The graph pooling at the last layer of GNN gathers the global information from the whole graph. The details of the model are in Appendix A. The architecture is shown in Fig.1.

3 Experiments

The dataset used is the SeasFire Datacube (Karasante et al., 2023), a global dataset spanning 21 years, featuring an 8-day temporal and $0.25\,\mathrm{deg}$ spatial resolution, containing crucial information on seasonal wildfire drivers, targets, and masks. We select three local weather variables Temperature at 2 meters - Mean (T2m), Total precipitation (TP), Vapor Pressure Deficit (VPD), and three Oceanic Climate Indices (OCIs) known to influence the test area, including North Atlantic Oscillation (NAO), Arctic Oscillation Index (AO) (Müller-Plath et al., 2022), and Nino 3.4 Anomaly (Nino34_anom) (Brönnimann, 2007). The time lag is 10 months for OCIs and 39×8 days for local variables. The target variable is a binary map of the burned areas. Additionally, we narrow the spatial coverage to Europe and test two cases with biome types "Mediterranean" and "Boreal" according to the static features of GFED regions and biomes. The causal graph contains seven nodes with the target variable included. The $\mathcal{A}$ masks out edges and nodes related to the target variable to avoid label leakage. The NNs use 2003 to 2015 data for training, 2016 to 2017 for validation, and 2018 to 2019 for testing. We compare our proposed model to the following baselines: 1) Long short-term memory (LSTM) (Hochreiter & Schmidhuber, 1997). 2) Gated recurrent units (GRUs) (Cho et al., 2014). 3) GNN_CORR uses the correlation coefficient (CC)-based adjacency matrix computed from temporal features of variables. 4) GNN_FULL uses a fully connected graph as the adjacency matrix. The model's performance is evaluated using the Area Under the Precision-Recall Curve (AUPRC) and the Area Under the Receiver Operating Characteristic Curve (AUROC). We test models' forecasting performance eight days in advance in the Mediterranean, and 1, 2, $8 \times$ eight days in Boreal to explore their long-term capacity.

4 Results and Analysis

The model performance at the forecasting horizon of 8 days in the Mediterranean is listed in Table 1. The baseline AUPRC achieved by a Random classifier equals the fraction of positives (Saito & Rehmsmeier, 2015) in the dataset, which is around 1.1%. The causal GNN shows competitive performance with common time-series classification methods and improved performance over a fully connected and CC-based graph. This highlights the importance of removing spurious links during GNN training, where the redundant edges can lead to over-smoothed node features and degraded prediction accuracy. The prediction map Fig.2b, essentially looks like a fire danger map as in similar studies which approach fire danger forecasting as a classification task. It matches well the target burned areas in a given 8-day period of summer 2019, which is part of the test set. The model

Model	AUPRC (%) ↑	AUROC (%) ↑
Random classifier	1.1	50.0
LSTM	32.9	91.9
GRU	**34.6**	91.6
GNN_CORR	30.5	92.1
GNN_FULL	29.1	90.8
GNN_CAUSAL (Proposed)	**34.6**	**92.4**

Table 1: AUPRC and AUROC performance of the different models for $h = 8$ days in Mediterranean.

performance at different prediction horizons in Boreal is shown in Fig.2a. The proportion of positive samples in this area is 0.0737%, a much more challenging case for all DL models. Our model achieves the best AUPRC at the short horizon. However, with the increasing horizons, the performance of Causal-GNN deteriorates with the rest of the models. The model's limited long-term forecasting capacity may be attributed to its static causal graph. Incorporating time-series graphs to account for time lags could potentially mitigate this issue.

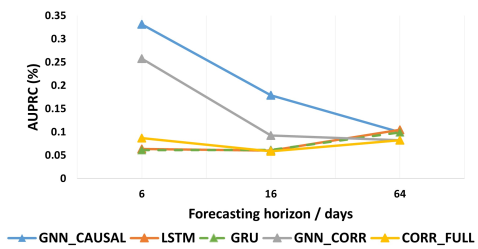

(a)

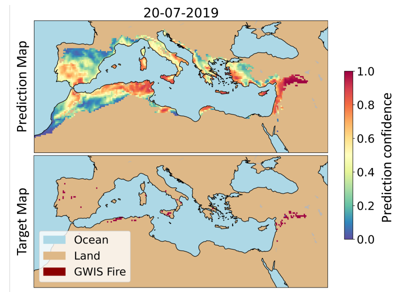

(b)

Figure 2: (a) AUPRC performance of the different models at forecasting horizon of 8, 16, 64 days in Boreal. (b) Causal-GNN predicted the sample fire danger map at eight days lead forecasting time in the Mediterranean.

Understanding the choice of Causal-GNN helps to refine the model and verify its physical consistency. Thus, we conduct SHAP analysis on positive test samples in the Mediterranean. From Fig.3a, we notice that high temperatures increase wildfire danger. In areas where the VPD is low ($<$0.7), the drier conditions correlate with an increased likelihood of wildfire. This relationship inverts while at the high VPD ($>$0.7) part. Figure 3b is the absolute SHAP value of OCIs at various lags averaged over samples. The increased value on large lags signifies the memory effects of large-scale atmospheric circulation patterns in driving future wildfires. For example, El Niño intensifies the wildfire danger, especially six to ten months in advance.

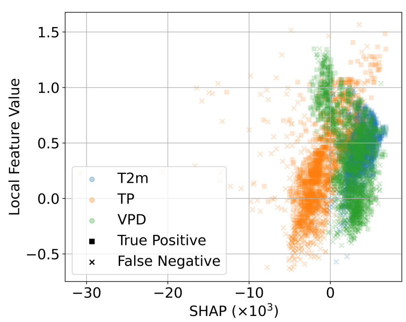

(a) SHAP value w.r.t local feature values.

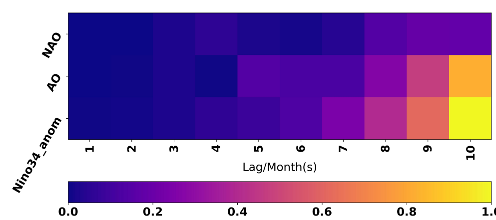

(b) Scaled absolute SHAP value of OCIs with changing lags.

Figure 3: (a) Square (cross) markers are True Positive (False Negative) samples. Positive (negative) SHAP value contributes to higher (lower) fire danger. (b) The warmer color shows a higher impact on the prediction.

5 Conclusion

This work proposes a DL framework that integrates the causal structure into the GNN training. The causal structure reveals the intricate interplay among variables and the temporal GNN, which takes the temporal feature of variables as nodes and weighted causal graph as connectivity, promoting the information exchange between variables that simulate both regional and larger-scale earth system dynamics. The evaluation of two cases with different vulnerable forest types shows promising results, especially when the dataset is highly imbalanced, indicating the robustness brought by causal knowledge. The gain over the CC-based method shows its efficacy in considering the synergistic effect and spurious link removal. xAI reveals the physically-consistent dependencies in the learned model. Our method paves the way to enhance process understanding and model trustworthiness.

Future efforts will focus on developing learnable causal graphs and examining the global variability. Additionally, we plan to explore regression of the burned area, with the goal to improve our understanding of different wildfire types and especially extreme events.

6 ACKNOWLEDGMENTS

The work of I. Prapas, I. Karasante and I. Papoutsis is funded by the European Space Agency in the context of the SeasFire project. The work of S. Zhao, Z. Xiong, and XX. Zhu is jointly supported by the German Federal Ministry of Education and Research (BMBF) in the framework of the international future AI lab "AI4EO – Artificial Intelligence for Earth Observation: Reasoning, Uncertainties, Ethics and Beyond" (grant number: 01DD20001), by German Federal Ministry for Economic Affairs and Climate Action in the framework of the "national center of excellence ML4Earth" (grant number: 50EE2201C), by the Excellence Strategy of the Federal Government and the Länder through the TUM Innovation Network EarthCare and by Munich Center for Machine Learning.

REFERENCES

Enric Batllori, Marc-André Parisien, Meg A. Krawchuk, and Max A. Moritz. Climate change-induced shifts in fire for Mediterranean ecosystems. *Global Ecology and Biogeography*, 22(10):1118–1129, 2013. ISSN 1466-8238. doi: 10.1111/geb.12065. URL https://onlinelibrary.wiley.com/doi/abs/10.1111/geb.12065. _eprint: https://onlinelibrary.wiley.com/doi/pdf/10.1111/geb.12065.

Stefan Brönnimann. Impact of el niño–southern oscillation on european climate. *Reviews of Geophysics*, 45(3), August 2007. ISSN 1944-9208. doi: 10.1029/2006rg000199. URL http://dx.doi.org/10.1029/2006RG000199.

Gustau Camps-Valls, Devis Tuia, XiaoXiang Zhu, and Markus Reichstein. *Deep learning for the Earth Sciences: A comprehensive approach to remote sensing, climate science and geosciences*. Wiley & Sons, 2021. ISBN 9781119646143. URL https://github.com/DL4ES.

Gustau Camps-Valls, Andreas Gerhardus, Urmi Ninad, Gherardo Varando, Georg Martius, Emili Balaguer-Ballester, Ricardo Vinuesa, Emiliano Diaz, Laure Zanna, and Jakob Runge. Discovering causal relations and equations from data. *Physics Reports*, 1044:1–68, 2023. ISSN 0370-1573. doi: https://doi.org/10.1016/j.physrep.2023.10.005.

Kyunghyun Cho, Bart Van Merriënboer, Caglar Gulcehre, Dzmitry Bahdanau, Fethi Bougares, Holger Schwenk, and Yoshua Bengio. Learning phrase representations using rnn encoder-decoder for statistical machine translation. *arXiv preprint arXiv:1406.1078*, 2014.

Emiliano Díaz, Jose E Adsuara, Álvaro Moreno Martínez, María Piles, and Gustau Camps-Valls. Inferring causal relations from observational long-term carbon and water fluxes records. *Scientific Reports*, 12(1):1610, 2022.

Bingbo Gao, Jianyu Yang, Ziyue Chen, George Sugihara, Manchun Li, Alfred Stein, Mei-Po Kwan, and Jinfeng Wang. Causal inference from cross-sectional earth system data with geographical convergent cross mapping. *nature communications*, 14(1):5875, 2023.

Sepp Hochreiter and Jürgen Schmidhuber. Long short-term memory. *Neural computation*, 9:1735–80, 12 1997. doi: 10.1162/neco.1997.9.8.1735.

Fernando Iglesias-Suarez, Pierre Gentine, Breixo Solino-Fernandez, Tom Beucler, Michael Pritchard, Jakob Runge, and Veronika Eyring. Causally-informed deep learning to improve climate models and projections. *arXiv preprint arXiv:2304.12952*, 2023.

Ilektra Karasante, Lazaro Alonso, Ioannis Prapas, Akanksha Ahuja, Nuno Carvalhais, and Ioannis Papoutsis. Seasfire as a multivariate earth system datacube for wildfire dynamics. *arXiv preprint arXiv:2312.07199*, 2023.

Spyros Kondylatos, Ioannis Prapas, Michele Ronco, Ioannis Papoutsis, Gustau Camps-Valls, María Piles, Miguel-Ángel Fernández-Torres, and Nuno Carvalhais. Wildfire danger prediction and understanding with deep learning. *Geophysical Research Letters*, 49(17):e2022GL099368, 2022.

Christopher Krich, Jakob Runge, Diego G. Miralles, Mirco Migliavacca, Oscar Perez-Priego, Tarek El-Madany, Arnaud Carrara, and Miguel D. Mahecha. Estimating causal networks in biosphere–atmosphere interaction with the pcmci approach. *Biogeosciences*, 17(4):1033–1061, February 2020. ISSN 1726-4189. doi: 10.5194/bg-17-1033-2020. URL http://dx.doi.org/10.5194/bg-17-1033-2020.

Fa Li, Qing Zhu, William J Riley, Lei Zhao, Li Xu, Kunxiaojia Yuan, Min Chen, Huayi Wu, Zhipeng Gui, Jianya Gong, et al. Attentionfire_v1. 0: interpretable machine learning fire model for burned-area predictions over tropics. *Geoscientific Model Development*, 16(3):869–884, 2023.

Scott M Lundberg and Su-In Lee. A unified approach to interpreting model predictions. *Advances in neural information processing systems*, 30, 2017.

Gisela Müller-Plath, Horst-Joachim Lüdecke, and Sebastian Lüning. Long-distance air pressure differences correlate with european rain. *Scientific Reports*, 12(1), June 2022. ISSN 2045-2322. doi: 10.1038/s41598-022-14028-w. URL http://dx.doi.org/10.1038/s41598-022-14028-w.

Judea Pearl. *Causality: Models, Reasoning, and Inference*. Cambridge University Press, September 2009. ISBN 9780521749190. doi: 10.1017/cbo9780511803161. URL http://dx.doi.org/10.1017/CBO9780511803161.

Adrián Pérez-Suay and Gustau Camps-Valls. Causal inference in geoscience and remote sensing from observational data. *IEEE Transactions on Geoscience and Remote Sensing*, 57(3):1502–1513, 2018.

M Lucrecia Pettinari and Emilio Chuvieco. Fire danger observed from space. *Surveys in Geophysics*, 41(6):1437–1459, 2020.

Ioannis Prapas, Spyros Kondylatos, Ioannis Papoutsis, Gustau Camps-Valls, Michele Ronco, Miguel-Ángel Fernández-Torres, Maria Piles Guillem, and Nuno Carvalhais. Deep learning methods for daily wildfire danger forecasting. *arXiv preprint arXiv:2111.02736*, 2021.

Ioannis Prapas, Nikolaos-Ioannis Bountos, Spyros Kondylatos, Dimitrios Michail, Gustau Camps-Valls, and Ioannis Papoutsis. Televit: Teleconnection-driven transformers improve subseasonal to seasonal wildfire forecasting. In *Proceedings of the IEEE/CVF International Conference on Computer Vision*, pp. 3754–3759, 2023.

Markus Reichstein, Michael Bahn, Philippe Ciais, Dorothea Frank, Miguel D Mahecha, Sonia I Seneviratne, Jakob Zscheischler, Christian Beer, Nina Buchmann, David C Frank, et al. Climate extremes and the carbon cycle. *Nature*, 500(7462):287–295, 2013.

Markus Reichstein, Gustau Camps-Valls, Bjorn Stevens, Martin Jung, Joachim Denzler, Nuno Carvalhais, and fnm Prabhat. Deep learning and process understanding for data-driven earth system science. *Nature*, 566(7743):195–204, 2019.

Jakob Runge, Sebastian Bathiany, Erik Bollt, Gustau Camps-Valls, Dim Coumou, Ethan Deyle, Clark Glymour, Marlene Kretschmer, Miguel D Mahecha, Jordi Muñoz-Marí, et al. Inferring causation from time series in earth system sciences. *Nature communications*, 10(1):2553, 2019a.

Jakob Runge, Peer Nowack, Marlene Kretschmer, Seth Flaxman, and Dino Sejdinovic. Detecting and quantifying causal associations in large nonlinear time series datasets. *Science advances*, 5 (11):eaau4996, 2019b.

Jakob Runge, Andreas Gerhardus, Gherardo Varando, Veronika Eyring, and Gustau Camps-Valls. Causal inference for time series. *Nature Reviews Earth & Environment*, 4(7):487–505, 2023.

Takaya Saito and Marc Rehmsmeier. The precision-recall plot is more informative than the roc plot when evaluating binary classifiers on imbalanced datasets. *PloS one*, 10(3):e0118432, 2015.

Bernhard Schölkopf, Francesco Locatello, Stefan Bauer, Nan Rosemary Ke, Nal Kalchbrenner, Anirudh Goyal, and Yoshua Bengio. Toward causal representation learning. *Proceedings of the IEEE*, 109(5):612–634, 2021.

Peter Spirtes, Clark Glymour, and Richard Scheines. *Causation, Prediction, and Search*. MIT Press, Cambridge, 2001.

George Sugihara, Robert May, Hao Ye, Chih-hao Hsieh, Ethan Deyle, Michael Fogarty, and Stephan Munch. Detecting causality in complex ecosystems. *science*, 338(6106):496–500, 2012.

Anastasios A Tsonis, Ethan R Deyle, Hao Ye, and George Sugihara. Convergent cross mapping: theory and an example. *Advances in nonlinear geosciences*, pp. 587–600, 2018.

Gherardo Varando, Miguel-Angel Fernández-Torres, and Gustau Camps-Valls. Learning granger causal feature representations. In *ICML 2021 Workshop on Tackling Climate Change with Machine Learning*, 2021.

Yunqian Wang, Jing Yang, Yaning Chen, Philippe De Maeyer, Zhi Li, and Weili Duan. Detecting the causal effect of soil moisture on precipitation using convergent cross mapping. *Scientific reports*, 8(1):12171, 2018.

Kun Zhang and Aapo Hyvarinen. On the identifiability of the post-nonlinear causal model. *arXiv preprint arXiv:1205.2599*, 2012.

A MODEL DETAILS AND HYPERPARAMETERS

The samples in the training and validation set are resampled so that the ratio of the number of negative samples (No fire) to positive samples (Fire) is 5 to 1. All learning rates are set as 1e-5 with a weight decay of 5e-6. Model weights are initialized using Xavier normalization. In the Causal-GNN, the temporal features of each input variable (channel-wise) are extracted by a single LSTM layer with the hidden state of dimension 256. The adjacency matrix is normalized to stabilize the graph learning. The temporal node feature is updated by a two-layer convolutional neural network with kernels $K \in \mathbb{R}^{256\times512\times1\times1}$ and $\mathbb{R}^{512\times256\times1\times1}$, following LayerNorm and LeakyReLU. The Graph Pooling averages node features, leading to the final classification layer. This is a single linear layer with dimensions (256 and 2) for binary classification tasks. Confidence is determined by the softmax function of the positive prediction, and it is used to visualize the fire danger map in Fig.2b.

For the baselines, LSTM and GRUs project the input feature to a dimension of 256. We utilize an adjacency matrix $\mathcal{A}$ for the fully connected graph, wherein all elements are set to 1, indicating complete connectivity. The correlation coefficient-based graph employs PyTorch's *corrcoef* function to calculate the similarity among variables within the temporal feature space. All performance scores are reported as the mean of three runs with different seeds.

B CAUSAL DISCOVERY

B.1 CAUSAL STATIONARITY

To prepare for the spatial-temporal stationary dataset, the input local variables are resampled to one-month intervals, and their mean is removed from the inputs. We test two cases over the Europe area, which are located between 25°N - 75°N, 13°W - 45°E. We use the biomes 3.0 area and biomes 9.0 area of the gfed region 6.0 (EURO) to consider the fuel types of Europe's Mediterranean and Boreal biomes. Their geographical extension is shown in Fig.4.

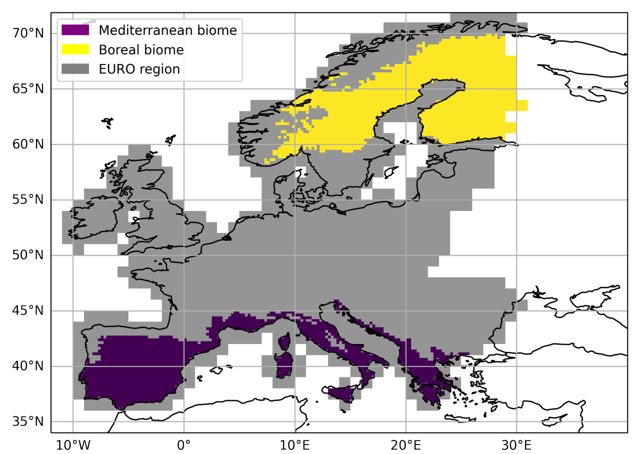

Figure 4: Test biomes in EURO region.

B.2 LINK ASSUMPTION

For the time series, we assume time order, the causal Markov condition, faithfulness, causal sufficiency, causal stationarity, and no contemporary causal effects (Runge et al., 2019b).

The link order is depicted in Fig.5.

B.3 CAUSAL GRAPHS

We compute causal graphs using PCMCI based on data from 2001 to 2019. The conditional independence test used is the one that accounts for partial correlations (ParCorr). The maximum time

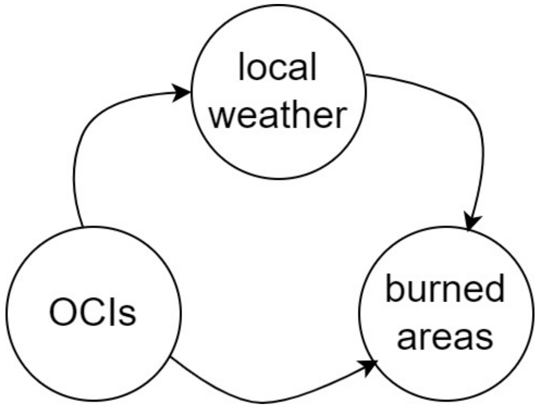

Figure 5: Causal order in PCMCI ParCorr independence test. The local weather includes temperature, total precipitation, and vapor pressure variables. The OCIs are the Arctic Oscillation, the North Atlantic Oscillation, and El-Niño in the 3.4 region. Here, the local weather acts as a mediator variable, explaining the relationship between an independent variable (OCIs) and a dependent variable (burned areas).

delay τ_{max} is six months. Significance level α at 0.05 is used to threshold the estimated matrix of p-values to get the graph. The derived causal graphs are shown in Fig.6.

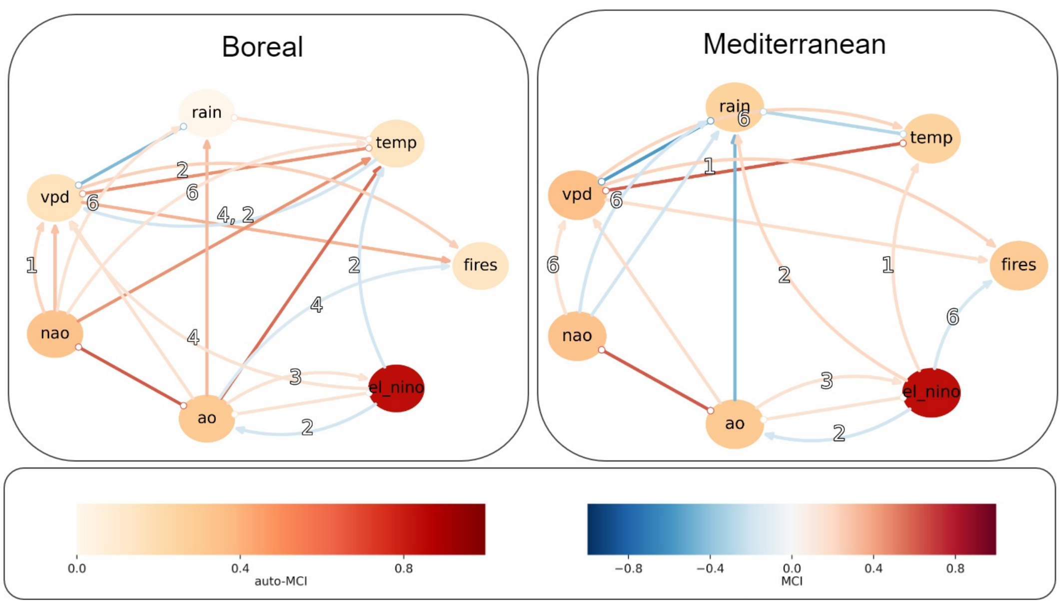

Figure 6: Causal graphs over Europe's Boreal and Mediterranean biomes. The color of the lines (MCI) of the causal links shows the strength of the relationship (positive for reds and negative for blues). The numbers in the arrows show their lagged relationship in months, if missing then the relationship is contemporaneous (lag 0). The arrows show the directionality, if any. The color of the nodes (auto-MCI) shows the autocorrelation of each variable with the time series.